

3 GERDA: Neutrinoless Double Beta Decay in ^{76}Ge

Laura Baudis, Giovanni Benato, Andreas James, Alexander Kish,
Michael Miloradovic, Rizalina Minghazeva, Manuel Walter

in collaboration with: INFN Laboratori Nazionali del Gran Sasso LNGS, Jagellonian University Cracow, Institut für Kern- und Teilchenphysik Technische Universität Dresden, Joint Institute for Nuclear Research Dubna, Institute for Reference Materials and Measurements Geel, Max Planck Institut für Kernphysik Heidelberg, Università di Milano Bicocca e INFN Milano, Institute for Nuclear Research of the Russian Academy of Sciences, Institute for Theoretical and Experimental Physics Moscow, Russian Research Center Kurchatov Institute, Max-Planck-Institut für Physik München, Dipartimento di Fisica dell'Università di Padova e INFN, Physikalisches Institut Eberhard Karls Universität Tübingen.

(GERDA Collaboration)

Some of the most important questions in modern particle physics can be addressed by investigating the elusive neutrinos. What is the nature of these fundamental particles, their mass scale and hierarchy, and what is the explanation of the observed matter-antimatter asymmetry in our universe? One of the prime tools in neutrino research is the search for neutrinoless double beta decay ($0\nu\beta\beta$). The discovery of this decay channel would prove that total lepton number is not conserved in nature and that neutrinos have a Majorana mass component. The world's highest lower limit on the half-life of the $0\nu\beta\beta$ decay of ^{76}Ge comes from the Germanium Detector Array (GERDA) experiment [1], as we describe in the following. A recent review of the field can be found in [2].

[1] Gerda Collaboration, K.-H. Ackermann *et. al*,
Eur. Phys. J. C **73** (2013) 2330.

[2] S. Dell'Oro, S. Marcocci, M. Viel, and F. Vissani,
Neutrinoless double beta decay: 2015 review,
arXiv[hep-ph]1601.07512.

3.1 The GERDA experiment

The GERDA experiment at the Laboratori Nazionali del Gran Sasso (LNGS) searches for the $0\nu\beta\beta$ decay using high-purity germanium diodes, isotopically enriched in ^{76}Ge [3]. These act simultaneously as the detector and source material. The germanium detectors are submerged in liquid argon (LAr). A water Cherenkov veto surrounds the LAr cryostat, and allows us to reject interactions from cosmic muons.

In the first stage of the experiment (Phase I), which lasted from 2011 to 2013, ten HPGe detectors with an active mass of 15 kg were used, resulting in a total exposure of 21.6 kg·y. A tenfold lower background than in previous experiments was obtained, with $1 \cdot 10^{-2}$ events/(keV · kg · y) at the Q-value of the decay ($Q_{\beta\beta}$). No $0\nu\beta\beta$ -decay signal was observed in Phase I, and a lower limit of $T_{1/2}^{0\nu\beta\beta} > 2.1 \times 10^{25}$ y at 90% C.L. for the half-life of the decay was obtained [4].

[3] Gerda Collaboration, M. Agostini *et. al*,
Eur. Phys. J. C **75** (2015) 39.

[4] Gerda Collaboration, M. Agostini *et. al*,
Phys. Rev. Lett. **111** (2013) 122503.

3.2 GERDA Phase II

During the upgrade of the experiment (Phase II, see Fig. 3.1), new, enriched Broad Energy Germanium (BEGe) detectors were built and extensively tested [3], and an active LAr veto system was installed at LNGS. The aim of this stage is to reach a sensitivity of $T_{1/2} = O(10^{26})$ y with a background index (BI) of 10^{-3} events/(keV·kg·y) after an exposure of 100 kg·y.

In the spring of 2015, the assembly of the upgraded detector array started, by mounting pairs of BEGe detectors in their new, low-background holders. It culminated with the mounting of all 40 detectors into the LAr cryostat, arranged in 7 strings (see Fig. 3.2). Each string is surrounded by a so-called *nylon mini-shroud* enclosing either 3 coaxial or 8 BEGe detectors. Only one string is composed of 6 BEGe's and 1 coaxial diode. The purpose of the mini-shrouds is to physically block ^{42}K ions, produced in ^{42}Ar decays in LAr, to reach the surface of the diodes and contribute to the background through β -decays. By December 2015, all the detectors were installed and characterised, and the Phase II data taking of GERDA started. We have contributed to the tests of the BEGe detectors, to the liquid argon veto [5] and to the calibration system hardware and software. We are now focussed on the physics data analysis.

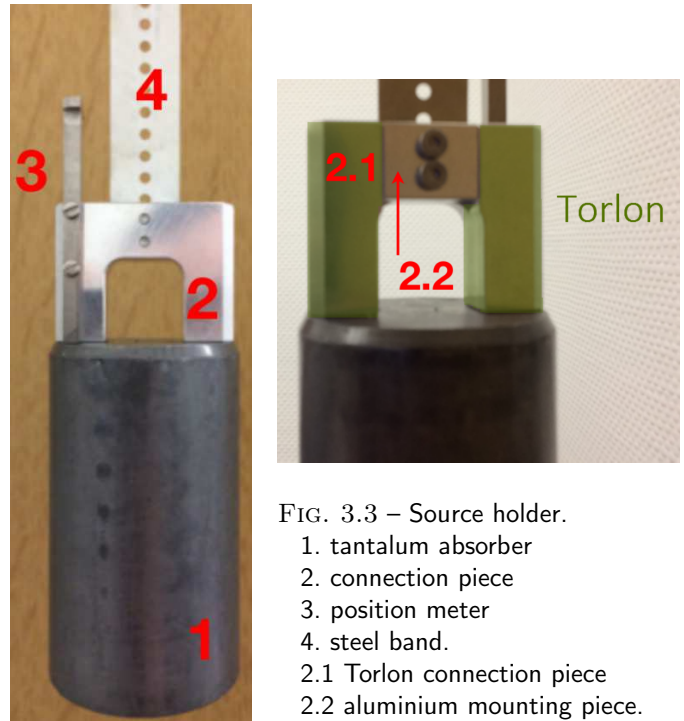
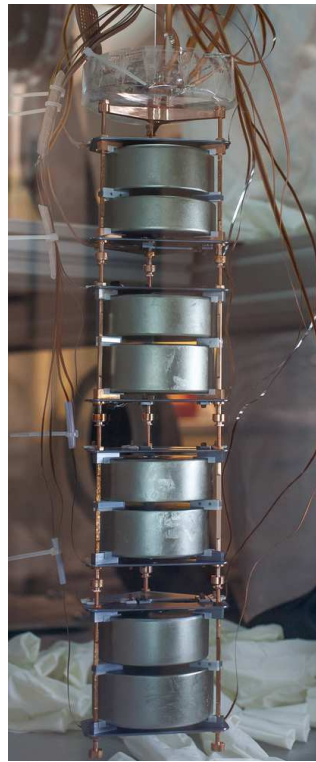
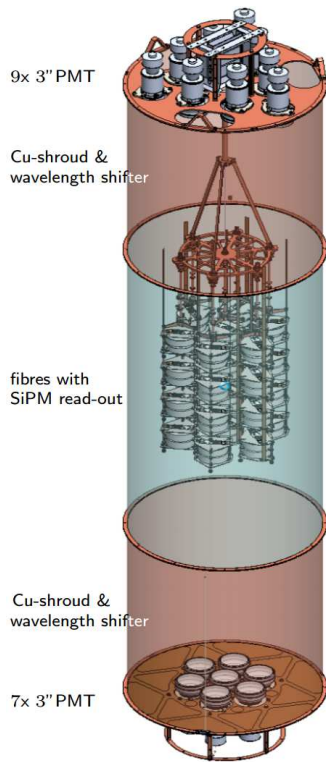


FIG. 3.3 – Source holder.

1. tantalum absorber
2. connection piece
3. position meter
4. steel band.
- 2.1 Torlon connection piece
- 2.2 aluminium mounting piece.

12

FIG. 3.1 – Schematic view of the GERDA Phase II germanium detector array and the surrounding liquid argon veto.

FIG. 3.2 – One of the GERDA Phase II strings containing eight broad-energy germanium detectors.

3.2.1 The Phase II calibration system

We have upgraded the three calibration systems that we had constructed and operated for GERDA Phase I [6]. We also produced new, low-neutron emission sources, in collaboration with PSI, and characterised these at the University of Zürich and at LNGS [7]. After the initial upgrade, we performed a modification of the ^{228}Th source holders, as shown in Fig. 3.3. The aluminium connection piece of the tantalum absorber was replaced with Torlon (polyamide-imide) to insulate it from the stainless steel band. We thereby prevented an observed high voltage instability in several germanium detectors.

We are currently acquiring 1-2 energy calibration runs per week, using the three ^{228}Th -sources. The purpose of the calibration procedure is to perform the energy and pulse shape calibration of all germanium detectors, and to monitor their energy resolution and energy scale stability in time.

3.2.2 Phase II calibration software

We have developed new calibration software tailored to the Phase II requirements. We have unified the code with all other packages used in the GERDA-ADA analysis framework (GERDA-Advanced-Analysis). We made major modifications to the program front-end. To handle and extract all relevant calibration information for each diode, the program now receives as input the detector and string settings, as well as the list of quality cuts which have to be applied to a given run. Since this part of the code also provides the interface between user and the executable program, it is flexible and intuitive for the user.

A new configuration file of quality cuts was developed which can be applied to all data types (background, calibration, physics run) in a similar fashion. The program can now use the class *TTreeFormula* of the ROOT analysis package. For this purpose, a new interface class to handle and apply the required cuts was developed. The calibration data is now loaded through key identifiers that allow the software to reconstruct the file system path in a performance optimised directory structure. Through dedicated key lists, all the resolved ROOT files are loaded in parallel. This procedure is now unified through all the layers of the Phase II data processing structure.

All these modifications have already been included into the latest, stable GERDA-ADA version.

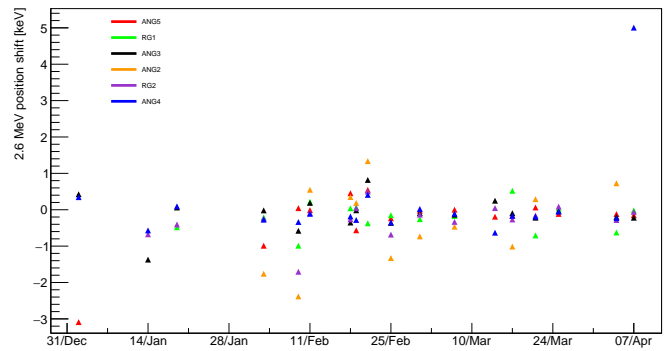
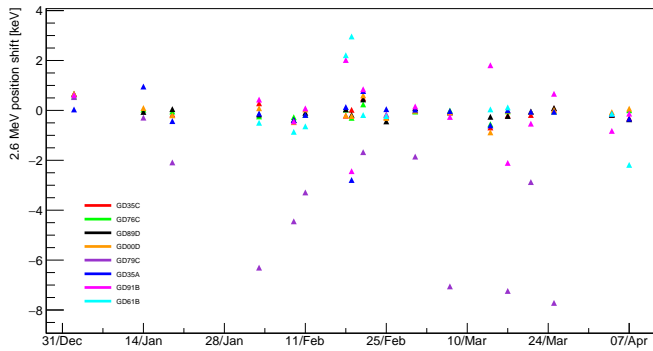


FIG. 3.4 – Coaxial (left) and BEGe (right) detector energy scale stability during the initial Phase II data taking. The relative shift in the position of the full energy peak at 2.6 MeV from the ^{208}Tl decay is quantified.

3.2.3 Phase II calibration data analysis

Using the calibration data, the energy scale and the resolution of the diodes can be monitored. Figure 3.4 shows the energy scale stability for coaxial and BEGe detectors, for calibration runs between December 2015 and April 2016. The energy scale is determined from the position of the full energy peak at 2.6 MeV from ^{208}Tl . Most coaxial detectors (6 out of 9) and most BEGe detectors show a stable behaviour. The BEGe detector GD79C revealed a high leakage current during data taking and was selected only for coincident events with multiple detectors.

The calibration data allowed an accurate study of possible shifts in the energy scale, needed in the final analysis. For this purpose, the energy gain stability both during the calibration runs, and during the actual physics runs (using a pulser) was investigated. Runs with instable detector operation are still under review.

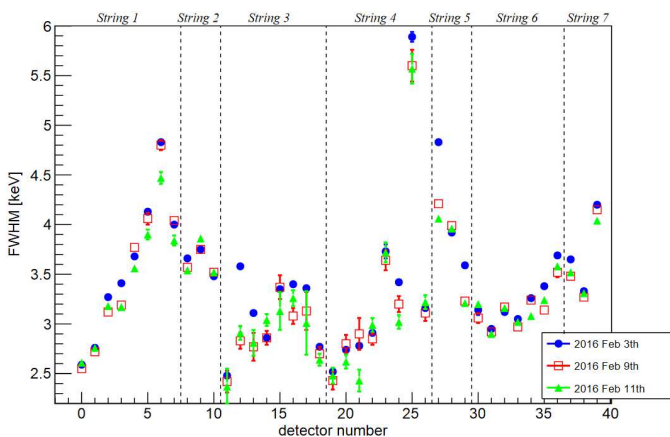


FIG. 3.5 – Energy resolution (at FWHM) of the 2.6 MeV γ -line of ^{208}Tl for 3 calibration runs and all 40 detectors. The vertical lines indicate the string boundaries.

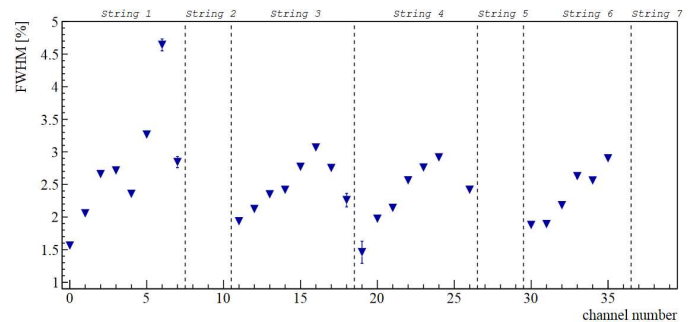


FIG. 3.6 – Resolution of the pulse shape analysis parameter A/E for BEGe detectors (strings 1, 3, 4 and 6). Several calibration runs are added in this analysis. The channel number is identical to the one shown in Fig. 3.5.

3.2.4 Phase II detector performance

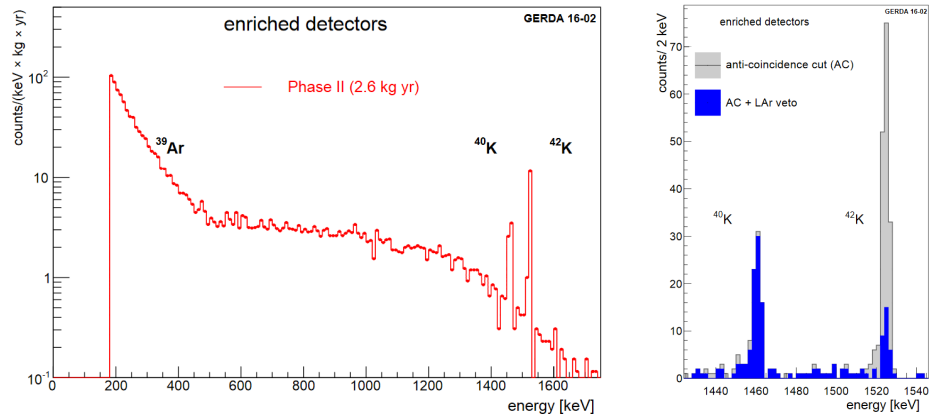
An example of the spectroscopic performance of all 40 germanium detectors (30 BEGe and 10 coaxial diodes) is shown in Fig. 3.5 for the 2.6 MeV calibration line. Most detectors have an energy resolution (at FWHM) below 4 keV, superior to the Phase I performance of 4.3 keV [8]. For BEGe detectors, the top detectors in a string (lowest channel number in each group) exhibit the highest resolution. This might be caused by larger stray capacitances due to the increasing cable length for the lower detectors. The average BEGe resolution at 2.6 MeV is 3.2 keV compared to 2.8 keV during Phase I.

The A/E parameter, with A the area of the charge pulse and E the energy, allows to reject surface events and multiple interactions in a given diode [9]. The A/E resolution of events in the double escape peak of the 2.6 MeV gamma is shown in Fig. 3.6. Cuts on A/E remove about 15% of the total number of events in a calibration run.

3.2.5 The liquid argon veto and physics data

The LAr veto, new in Phase II (see Fig. 3.2), is a scintillating detector equipped with photomultiplier tubes

FIG. 3.7 – Left: background energy spectrum in the Ge detectors, for an exposure of 2.6 kg y. Right: γ -lines from ^{40}K decay in material close to the diodes, and from ^{42}Ar with and without argon veto.



(PMTs) and silicon photomultipliers (SiPMs). All channels are working and their performance is stable in time. Figure 3.7 shows the observed background energy spectrum below 1.8 MeV and the effect of the argon veto on the γ lines around 1.5 MeV. Clearly visible is the suppression of the ^{42}K peak at 1525 keV: if the β -decay occurs at some distance from the detectors (e.g. at the mini-shroud surface), the electron deposits energy in the argon too and the event can be vetoed.

The observed ^{40}K peak at 1461 keV is from electron capture and not accompanied by an energy deposition in the argon. Both peaks, however, contain to a large fraction multi-site events (MSEs) which can be rejected by pulse shape discrimination (see Fig. 3.8). Single site events (SSEs) – similar to double beta decays of ^{76}Ge with neutrino emission – are located in a band around $A/E = 1$. These events dominate in an energy range around 1 MeV. MSEs and events on the n+ contact surface have $A/E < 1$, visible for the two γ lines mentioned above. Events at the p+ contact can be clearly identified by high A/E values. α decays originating from ^{210}Po with an endpoint of 5.3 MeV are also visible in the figure.

The accumulated statistics for the enriched detectors is about 4.8 kg·y, though not all might be used for physics analysis later on. The background level before using the active argon veto and event discrimination based on pulse shape analysis is similar to the one in Phase I [10].

- [9] Gerda Collaboration, M. Agostini *et. al*, Eur. Phys. J. C 73 (2013) 2583.
 [10] Gerda Collaboration, M. Agostini *et. al*, Eur. Phys. J. C 74 (2014) 2764.

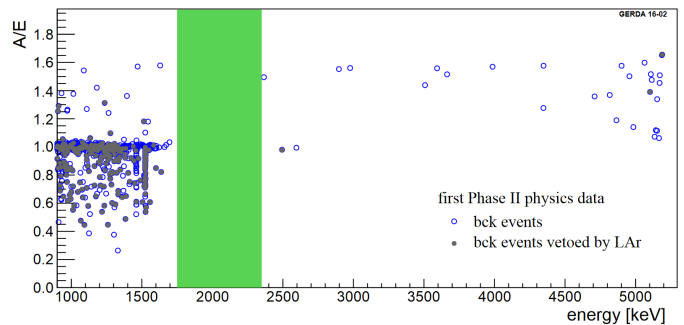


FIG. 3.8 – A/E versus E for the BEGe detectors. A 400 keV band around $Q_{\beta\beta}=2039$ keV is blinded.

3.3 Outlook

The entire array of 40 HPGe detectors was mounted successfully. They can be biased well above depletion voltage (except detector GD79C) and all readout channels are working. The active liquid argon veto is working well too, showing stable performance in time. Since the end of January 2016, the data is blinded, i.e. events in the window $Q_{\beta\beta} \pm 25$ keV are not reconstructed to ensure an unbiased analysis. We are now strongly involved in the analysis of the GERDA Phase II data. A first estimate of the remaining background at $Q_{\beta\beta}$ will be available in late spring, and unblinding is planned for summer 2016. Depending on the observed background level, some hardware modifications such as new readout cables from cleaner material (already available and screened) could be scheduled after a first physics result.

- [5] L. Baudis, G. Benato, R. Dressler, F. Piastra, I. Usoltsev and M. Walter, JINST 10 (2015) P09009.
 [6] L. Baudis, A.D. Ferella, F. Froberg, and M. Tarka, Nucl. Instrum. Meth. A729 (2013) 557-564.
 [7] L. Baudis, G. Benato, P. Carconi, C.M. Cattadori, P. de Felice, K. Eberhardt, R. Eichler, A. Petrucci, M. Tarka, and M. Walter, JINST 10 (2015) no.12, P12005.
 [8] Gerda Collaboration, M. Agostini *et. al*, Eur. Phys. J. C 75 (2015) 255.